# Inductance calculation for 3D microsolenoids with single-layer coils

LIU Keyin, YANG Qing, CHEN Feng, ZHAO Yulong,
MENG Xiangwei, SHAN Chao, LI Yanyang

(*State Key Laboratory for Manufacturing System Engineering & Key Laboratory of Photonics Technology for Information of Shaanxi Province*, *Xi'an Jiaotong University*, *Xi'an*, 710049, *China*)

**Abstract**: Three-dimensional (3D) single-layer microcoils have always been a key element for electromagnetic systems; but they lack an easy and accurate method to calculate the inductance value for their complex 3D micro-structures. This paper employed a curve-fitting process to obtain the associated equation for the inductance value and geometric parameters based on the simulation results. The correction factors regarding helical pitch and wire diameter were reviewed, which are used for compensation in the Nagaoka formula. The simulation process numerically simulated the performance of the 3D microcoils using a FEM electro-magnetic-coupled analysis method. Comparison of the simulated inductance value and the Nagaoka formula was undertaken, which shows that the helical pitch and wire diameter contribute a main role in the calculation error. The derived formula was expressed in a concise form to precisely calculate the inductance value of 3D microsolenoids with single-layer coils.

**Key words**: Three-dimensional microsolenoids, finite element simulation, curve fitting, inductance calculation

## 1 Introduction

Three-dimensional (3D) microsolenoids with single-layer microcoils are a key element in a various of microsystems, including integrated circuits (IC), microfluidic systems, microwave applications and microelectromechanical systems (MEMS)[1-5]. Compared to large-scale solenoids, 3D microsolenoids are usually equipped with a sparse structure, and have a large ratio of helix pitch and wire diameter to coil radius. However, there lacks an easy and precise method to calculate the inductance value of complex 3D microsolenoids, which is a crucial solenoid parameter. Analytical investigation of microsolenoids currently mainly concentrates on two-dimensional (2D) planar microspirals, which correlates with the available fabricating technologies[6-10]. Performance prediction of 3D microsolenoids mainly depends on an empirical formula or scalar analysis using the finite element method (FEM) based on simplified models[11-17]. Some other analytical methods have also been reported which focus on 3D microsolenoids, but these methods consist of a tedious and complicated calculation process[18-22]. All these methods have limitations preventing precise calculation of the properties of 3D micro-scale solenoids, since they do not take into consideration the unique 3D geometry configuration. Most calculation formulas are valid for the current sheet approximation, where the electric current flows in an indefinitely thin surface around the coil diameter with negligible separation between turns. This is the same as assuming that the coil is wound with an indefinitely thin tape with negligible separation between turns. If the separation between turns and wire diameter is not small, a correction should be applied to these calculation methods. In addition, most reported formulas cannot be applied to 3D microsolenoids that are not straight.

In other recent studies, we have fabricated 3D microsolenoids in fused silica with a femtosecond-laser-based microsolidifying method[23-24]. In this paper, a 3D FEM simulation and curve-fitting method was employed to analyze the 3D microsolenoids. 3D microsolenoids with different geometric parameters or configurations were modeled and numerically simulated. The simulation process involved electromagnetic-coupled FEM-3D-vector calculation using the ANSYS software. Then, a curve-fitting method was employed to obtain the associated equations for the inductance value and geometric parameters. The fitting equations described here were deduced from the simulation results; and the derived goodness-of-fit value was proposed to justify these equations. The derived formula was preliminarily validated by measuring the inductance of 3D microsolenoids fabricated by the femtosecond-laser-based microsolidifying technology.

## 2 Analysis and evaluation

### 2.1 Analytic comparison

The calculating formula was derived from the simulation results using a curve-fitting method. In the simulation process, 3D microsolenoids were firstly modeled based on their complex 3D configurations. A direct current of 0.2 A was then applied to the 3D microsolenoids to conduct the simulation process and calculate the electromagnetic performance, as shown in Fig. 1. The stored magnetic co-energy of 3D microsolenoids was subsequently simulated based on the configuration of the 3D microsolenoids. A simulation-based co-energy calculation method was used to evaluate the inductance of the 3D microsolenoids, using the formula:

$$L = \frac{2W_L}{A^2} \quad (1)$$

where $L$ is the inductance value, $W_L$ is the stored magnetic co-energy and $A$ is the current value through the microcoil. The calculated results were compared with the Nagaoka formula[11] which has been widely used to calculate the inductance of short cylindrical air-core coils:

$$L = \frac{K\mu_0 N^2 \pi D^2}{4I} \quad (2)$$

where $\mu_0$ is the permeability of free space ($4\pi 10^{-7}$ H/m), $N$ is the number of coils of the solenoid, $D$ is the solenoid diameter, $I$ is the length of the solenoid and $K$ is the shape factor, which is related to the ratio of solenoid diameter to solenoid length ($D/I$). The Nagaoka formula has the drawback of requiring a list of tabulated values for different $D/I$ values. A relative error was used to show the calculation accuracy of Nagaoka formula compared with the simulation results.

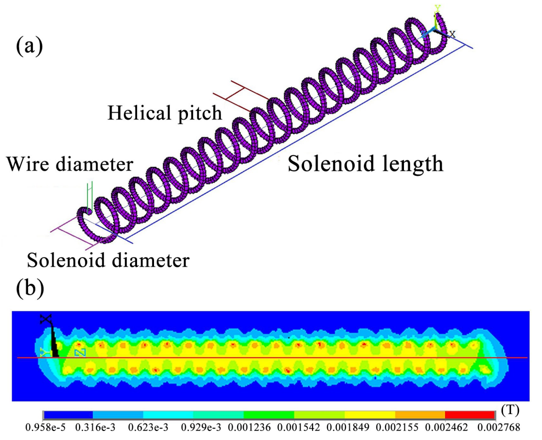


**Fig. 1 Simulation results of the 3D single-layer coils: (a) schematic diagram, (b) magnetic field distribution with a direct current of 0.2 ampere. The geometric parameters are: number of coils 20, helical pitch 125 μm, mean solenoid diameter 200 μm and wire diameter 30 μm. The solenoid length is determined by the number of coils and the helical pitch as 2.5 mm.**

$$Error_{relative} = \frac{|L_{simulation} - L_{calculation}|}{L_{simulation}} \quad (3)$$

Although the results of simulation and calculation coincide with each other well at small helical pitch to solenoid diameter ratios ($H/D$), the Nagaoka formula is not suitable for sparse solenoids that a significant deviation is identified between the Nagaoka formula and simulation results when the wire diameter and spacing between turns is large, as shown in Fig. 2 and Fig. 4. Here, the FEM-3D-vector analysis concentrates more on the microsolenoid's geometry and almost completely approaches real 3D microsolenoids.

### 2.2 Structure analysis

In order to conduct optional design and performance prediction of 3D microsolenoids, it is necessary to firstly deduce associated formulas. However, owing to the complex 3D structure, the precise theoretical formulas relating to the microsolenoid's properties are difficult to derive. But approximate formulas can be obtained using a combination of 3D-FEM-vector calculation and curve fitting.

According to empirical formulas of finite length solenoids, inductance is a function of each individual structural dimension variable. Therefore, the functional relationships of 3D microsolenoids are likely to be similar to the empirical formulas, and correction factors can be applied to the empirical Nagaoka formula for more precise calculation. Consequently, the functional forms can be set as follows:

$$L=\gamma \cdot \delta(\frac{H}{D}) \cdot \varepsilon(\frac{d}{D}) \cdot \sigma(\frac{D}{I}) \cdot \frac{\mu_0 N^2 \pi D^2}{4I} \tag{4}$$

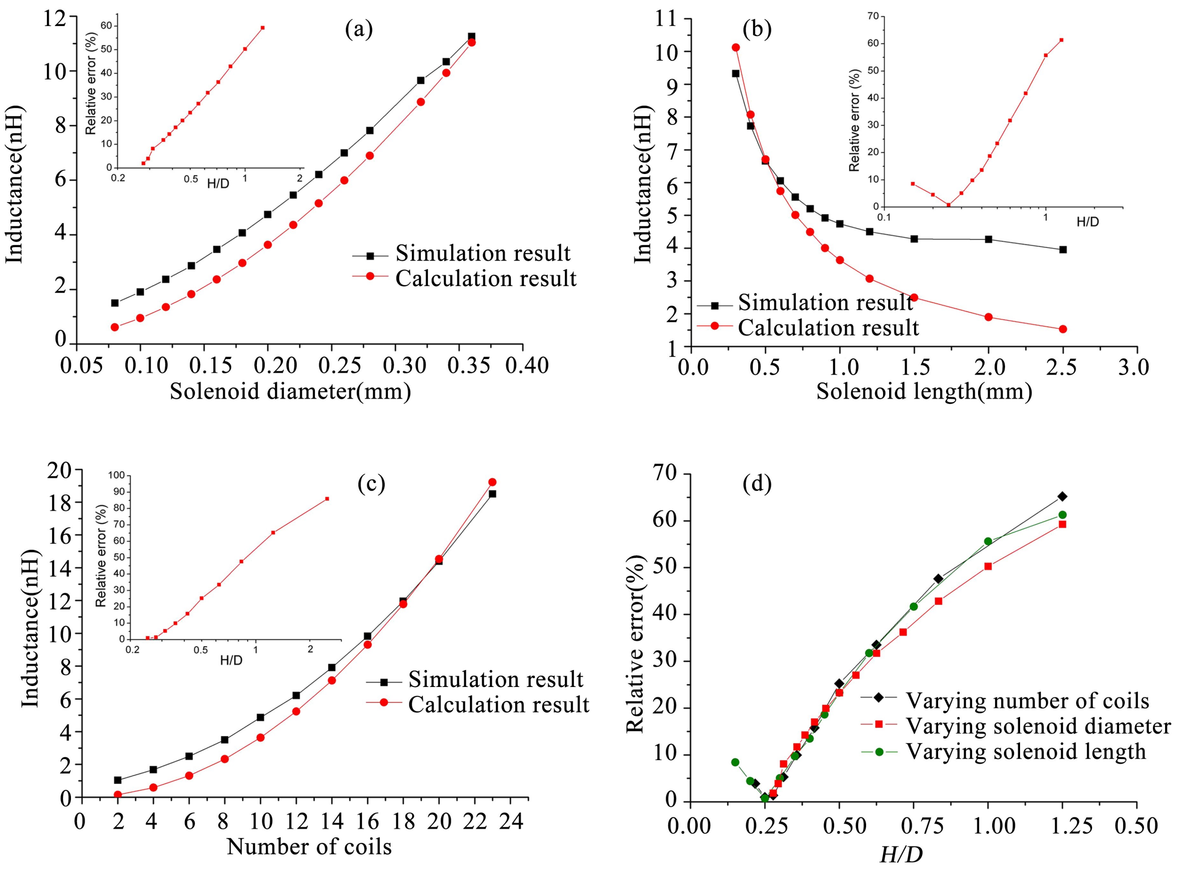


**Fig. 2 Simulation results of the FEM-3D-vector analysis and Nagaoka formula calculation: (a) solenoid diameter is varied from 80~360 μm, keeping the number of coils at 10, wire diameter at 10 μm and solenoid length at 1 mm, (b) solenoid length is varied from 0.2~2.5 mm, keeping number of coils at 10 , wire diameter 10 at μm and solenoid diameter at 200 μm, (c) varying number of coils is varied from 2~23, keeping solenoid length at 1 mm , wire diameter at 10 μm and solenoid diameter at 200 μm, (d) relationship between the relative error and the ratio of helical pitch to solenoid diameter (*H/D*).**

where $\delta(\frac{H}{D})$ is the shape factor related to the ratio of helical pitch to solenoid diameter ($H/D$), $\varepsilon(\frac{d}{D})$ is the shape factor related to the ratio of wire diameter to solenoid diameter ($d/D$), $\sigma(\frac{D}{I})$ is the shape factor related to the ratio of solenoid diameter to solenoid length ($D/I$), which is derived from the Nagaoka shape factor and $\gamma$ is the modifying factor, which is related to the curve-fitting boundary conditions. The similarity between these equations and the simulation curves is expressed by the residual curves. The residual curve is formed by residual error points that reflect the difference between a group of stimulated values and their arithmetical mean.

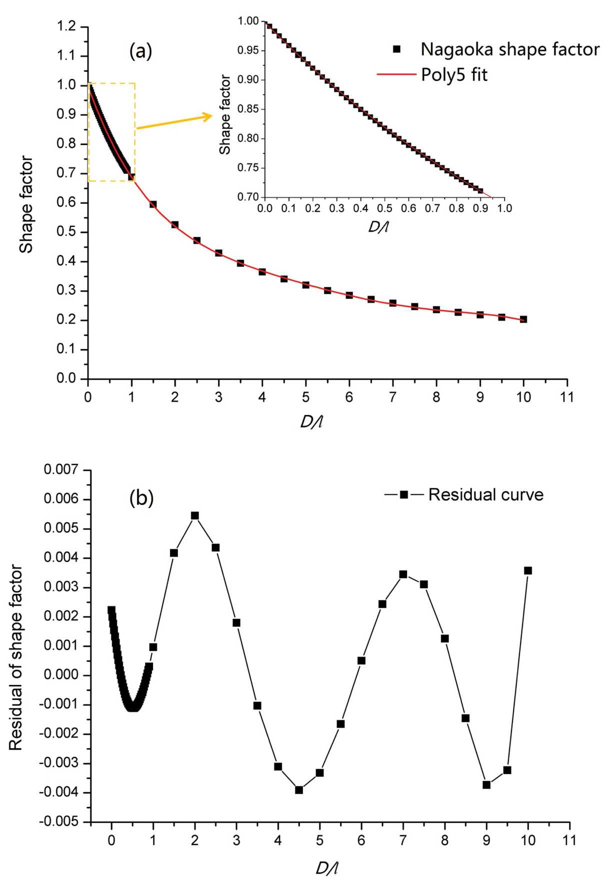


**Fig. 3 (a) Relationship of the shape factor and the ratio of solenoid diameter to solenoid length ($D/I$), (b) the residual curve of the shape factor relating to $D/I$.**

Firstly, the Nagaoka shape factor table was simplified into the shape factor $\sigma(\frac{D}{I})$. The shape factor $\sigma(\frac{D}{I})$ can be expressed as

$$\sigma(\frac{D}{I}) = a \times f_1(\frac{D}{I}) \tag{5}$$

where $f_1(\frac{D}{I})$ is the expression derived from the Nagaoka shape factor table, as shown in Fig. 3 and the coefficient $\sigma(\frac{D}{I})$ can be determined by the boundary condition: $\sigma(0)=1$. Thus, the expression $\sigma(\frac{D}{I})$ can be derived as

$$\sigma(\frac{D}{I})=1-0.4132(\frac{D}{I})+0.12102(\frac{D}{I})^2-0.02012(\frac{D}{I})^3+0.00168(\frac{D}{I})^4-5.5014\times10^{-5}(\frac{D}{I})^5 \tag{6}$$

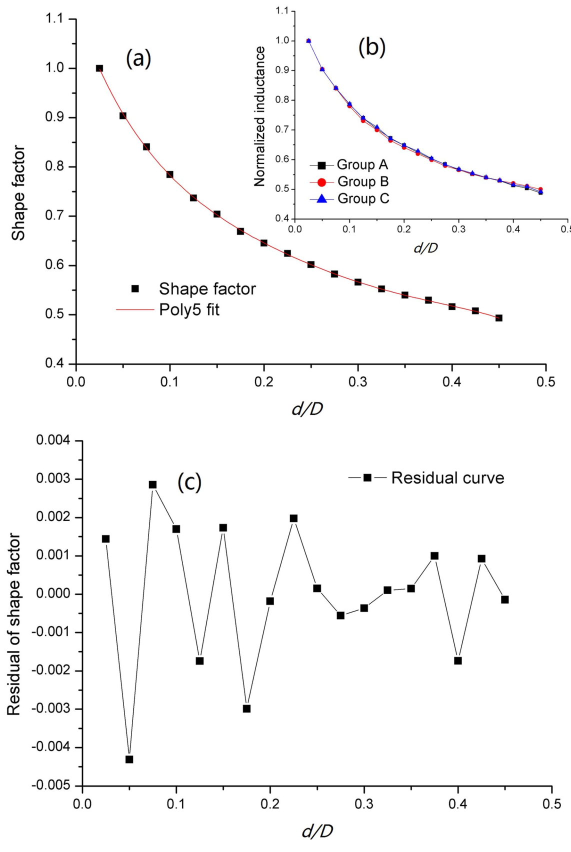


**Fig. 4 (a) Relationship of the normalized solenoid inductance and the ratio of wire diameter to solenoid diameter ($d/D$), and (b) normalized solenoid inductance for Group A: wire diameter is varied from 5 ~ 90 μm, keeping the solenoid diameter at 200 μm, number of coils at 10 and the solenoid length at 1 mm; Group B: wire diameter is varied from 5~90 μm, keeping the solenoid diameter at 200 μm, number of coils at 6 and the solenoid length at 1.2 mm; Group C: wire diameter is varied from 5 ~ 90 μm, keeping the solenoid diameter at 200 μm, number of coils at 12 and the solenoid length at 1.08 mm. (c) the residual curve of inductance relating to $d/D$.**

The coefficient $a$ can be calculated as $a = 1/0.99777$, determined by the boundary condition: $\sigma(0)=1$.

The influence of the wire diameter on the inductance value was studied as three independent groups of geometric parameters, as shown in Fig. 4 (b). The inductance value of the microsolenoid can be normalized according to the formula

$$L_{normalization} = L_{simulation}/L\frac{d}{D} = 0.025 \quad (7)$$

From Fig. 4(b), we observe that the influence of the wire diameter on the inductance value is independent of the other geometric parameters. Thus, the shape factor $\varepsilon(\frac{d}{D})$ can be expressed as

$$\varepsilon(\frac{d}{D}) = b \times f_2(\frac{d}{D}) \quad (8)$$

where $f_2(\frac{d}{D})$ is the expression derived from the mean value of the normalized inductance when varying the ratio of wire diameter to solenoid diameter ($d/D$), as shown in Fig. 4(a). The coefficient $b$ is determined by the boundary condition: $\varepsilon(0) = 1$. Thus, the expression $\varepsilon(\frac{d}{D})$ can be derived as

$$\varepsilon(\frac{d}{D}) = 1 - 4.7893(\frac{d}{D}) + 25.2120(\frac{d}{D})^2 - 84.8592(\frac{d}{D})^3 + 152.3190(\frac{d}{D})^4 - 109.8087(\frac{d}{D})^5 \quad (9)$$

The coefficient $b$ is calculated as $b = 1/1.11564$, determined by the boundary condition: $\varepsilon(0)=1$.

The calculation inductances in Fig. 2(a-c) are then updated by multiplying the Nagaoka formula calculation results with the shape factor $\varepsilon(\frac{d}{D})$:

$$L=\varepsilon(\frac{d}{D}) \cdot =\frac{K\mu_0 N^2 \pi D^2}{4l} \quad (10)$$

The relative error between the simulation results and calculation results is then recalculated using formula 3 and compared with that in Fig. 2(d), as shown in Fig. 5. The updated relative errors of the three independent simulation processes are more consistent with each other compared with the relative error values in Fig. 2(d). This is due to the influence of the variation of $d/D$ values. The $d/D$ value (0.028~0.25) increases with $H/D$ value (0.28~1.25) in the simulation process where the solenoid diameter is varied, but remains constant in the other two simulation processes. Thus, the increase of $d/D$ with $H/D$ results in a decrease in the solenoid inductance. In addition, the relative error lines almost coincide with each other, which means that the $H/D$ ratio is an independent factor which influences the calculation accuracy of the Nagaoka formula.

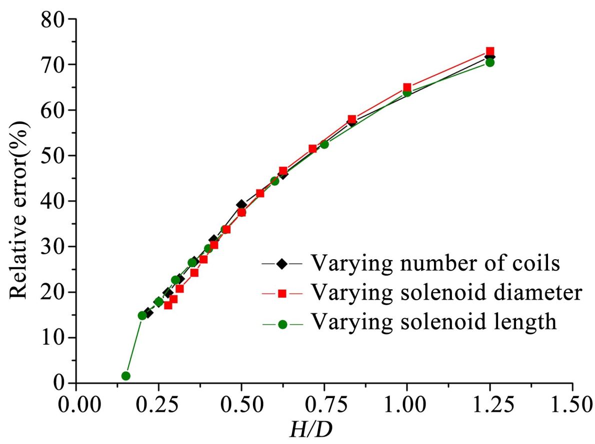


**Fig. 5 Updated relative error related to *H/D* between the simulation results and calculation results.**

The shape factor $\delta(\frac{H}{D})$ can be expressed as

$$\delta(\frac{H}{D}) = c \times f_3(\frac{H}{D}) \quad (11)$$

where $f_3(\frac{H}{D})$ is the expression derived from the calculated shape factor $\delta'(\frac{H}{D})$ using formula 12, the ratio of helical pitch to solenoid diameter $H/D$ is varied as shown in Fig. 6 and the coefficient $c$ is determined by the boundary condition: $\delta(0)=1$.

$$\delta'(\frac{H}{D}) = \frac{L_{simulation}}{\varepsilon(\frac{d}{D}) \cdot \frac{K\mu_0 N^2 \pi D^2}{4l}} \quad (12)$$

where $L_{simulation}$ is the simulation inductance, $\varepsilon(\frac{d}{D})$ is the shape factor related to the ratio of wire diameter to solenoid diameter $d/D$ and $\frac{K\mu_0 N^2 \pi D^2}{4l}$ is the Nagaoka calculation formula.

The expression $\delta(\frac{H}{D})$ can be derived as

$$\delta(\frac{H}{D}) = 1+0.23765(\frac{H}{D})+2.06850(\frac{H}{D})^2-0.91209(\frac{H}{D})^3+0.31440(\frac{H}{D})^4-0.04303(\frac{H}{D})^5 \quad (13)$$

The coefficient $c$ is calculated as $c=1/1.04194$, determined by the boundary condition: $\delta(0)=1$.

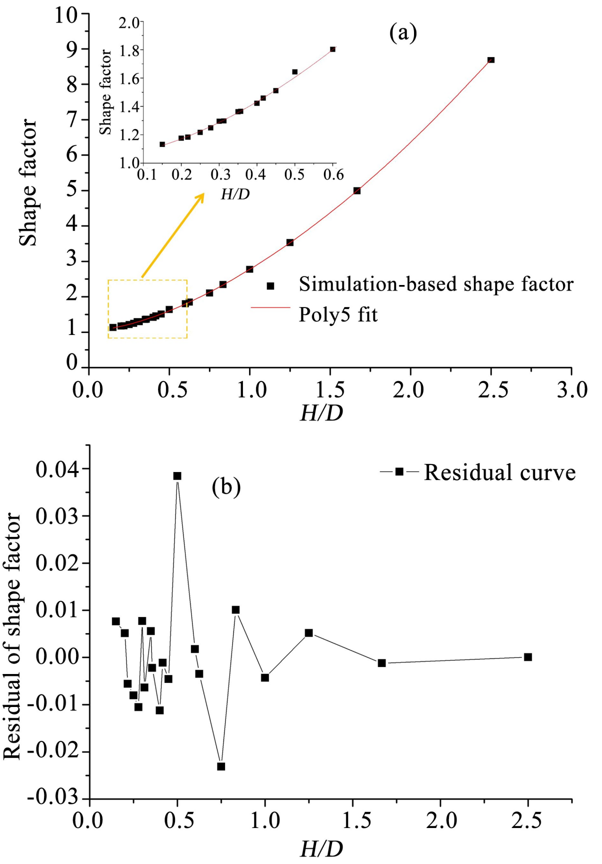


**Fig. 6 (a) Relationship of the calculated shape factor and the ratio of helical pitch to solenoid diameter (*H/D*), (b) the residual curve of the shape factor relating to *H/D*.**

The coefficients of determination $R^2$ and residual mean square were introduced to achieve the best goodness-of-fit, as shown in table 1. The mean square of residual error reflects the relative error. Similarly, it shows that the curve fits well when the value of $R^2$ gets closer to 1; in contrast, as the value gets closer to 0, the fit becomes less suitable.

As the coefficients $a$ and $c$ are independently determined by their boundary conditions, calculating errors are then introduced into the curve-fitting results. The modifying factor $Y$ is then employed to compensate the errors, calculated as

$$Y=\frac{1}{a \cdot c}=1.0396 \quad (14)$$

The modifying factor $Y$ reflects the curve-fitting accuracy. For the purpose of calculating inductances of ideal densely-wound uniform straight solenoids (wire diameter $d=0$, helical pitch $H=0$), the derived expression can be rewritten as

$$L=Y \cdot \sigma \frac{D}{I} \cdot \frac{\mu_0 N^2 \pi D^2}{4l} \quad (15)$$

As the modifying factor $Y$ is extremely close to 1, the derived expression is in close agreements with the Nagaoka formula to calculate inductances of ideal densely-wound uniform straight solenoids. Simultaneously, the modifying factor $Y$ can be defined as the shape factor related to the construction structure, as shown in Fig. 7. 3D microsolenoids of U shape and O shape were modeled and simulated using the FEM-3D-vector analysis method. The geometric parameters were kept the constant as the straight microcoil in Fig. 2. The inductance value for the straight microcoil, U-shape microcoil and O-shape microcoil is 7.04 nH, 6.897 nH and 7.345 nH respectively. The O-shape microsolenoid exhibits the largest solenoid inductance, because it is accompanied with the minimum magnetic flux leakage due to its circular structure. The modifying factor $Y$ for U shape and O shape microsolenoids can be estimated as 1.0185 and 1.0847 respectively.

**Table 1 Values of the coefficient of determination $R^2$ and residual mean square**

| $\varepsilon(\frac{d}{D})$ | $\delta(\frac{H}{D})$ | $\sigma(\frac{D}{I})$ | |
|---|---|---|---|
| Adjusted $R^2$ | 0.99981 | 0.99994 | 0.99994 |
| Residual mean square | $1.15563\times10^{-4}$ | $1.83542\times10^{-4}$ | $3.70057\times10^{-6}$ |

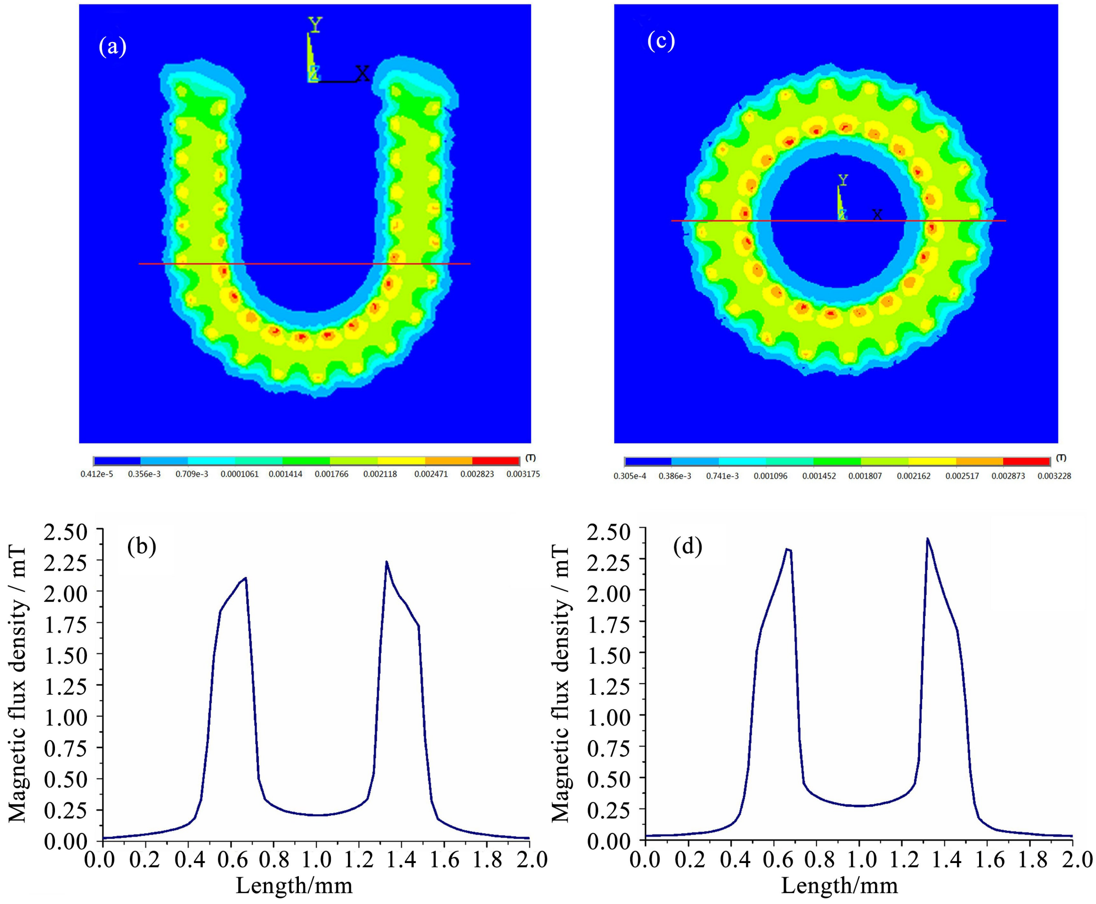


**Fig. 7 Magnetic flux density distribution of (a, b) O shape and (c, d) U shape microsolenoids. Geometric parameters: number of coils is 20, helical pitch is 125 μm, solenoid diameter is 200 μm, wire diameter is 30 μm and circle diameter is 800 μm.**

## 3 Experimental validation

The femtosecond-laser-based microsolidifying method is employed to fabricate the 3D microsolenoids by injecting liquid metal into helical microchannels in fused silica and solidifying the liquid metal[23-24]. The fabricated microsolenoid was packaged with a polydimethylsiloxane (PDMS) block and connected by two wire electrodes (length = 20 mm, wire diameter = 0.4 mm), as shown in Fig. 8. The geometric parameters of the microsolenoid were measured as: number of coils equals 20, helical pitch is ~125 μm, solenoid diameter is ~200 μm and wire diameter is ~30 μm. The inductance of wire electrodes can be calculated using the formula[16].

$$L=\frac{\mu_0 L}{2\pi}\left(in\left\{\frac{2L}{r}\right\}-0.75\right) \qquad (16)$$

where $\mu_0$ is the permeability of free space ($4\pi\times10^{-7}$ H/m), $I$ is the wire length and $r$ is the wire diameter. Thus, the total inductance value was calculated as ~39 nH. The inductance value was measured with an impedance analyzer, as shown in Fig. 8 (c). From the results, we observe that the derived formula can accurately predict the static inductance value of complex 3D microsolenoids.

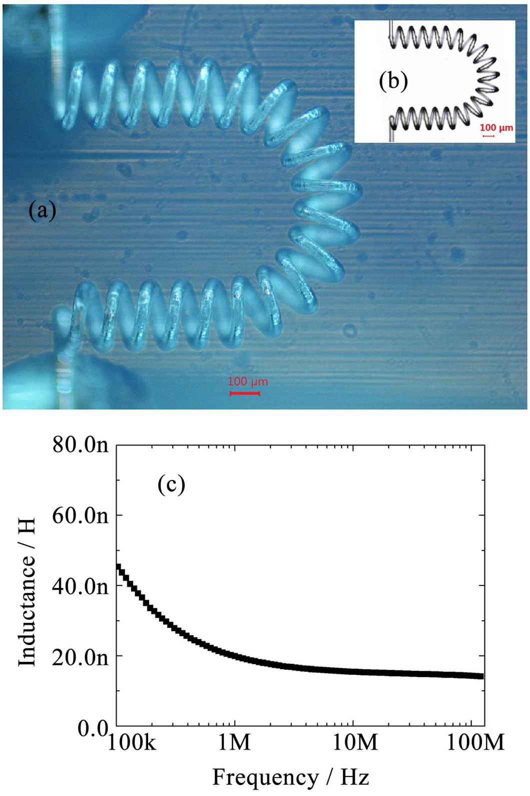


**Fig. 8 U-shape microsolenoids fabricated by the femtosecond-laser-based microsolidifying process and (b) the 3D microchannel before injecting metal, (c) measured inductance value**

We calculated the inductance value of a reported microcoil for on-chip NMR[2] using the deriv ed formula, and found that the simulation method can precisely calculate the inductance of 3D microsolenoids: the calculated inductance was ~38.1 nH according to the microcoil geometry in Fig. 1 of Ref. 2, while the measured inductance was 38 nH.

## 4 Conclusion

An easy and accurate inductance prediction method for complex 3D microsolenoids was proposed and studied in this paper. A FEM simulation method was employed to evaluate the properties of 3D microsolenoids in a close-to-actuality manner. A FEM-3D-vector simulation method was employed to evaluate the properties of 3D microsolenoids in a manner that was close to the actual real-world microsolenoid behavior. A curve-fitting process was then employed to obtain the associated equations for inductance value and geometric parameters based on the simulation results. Correction factors regarding geometric parameters of the helical pitch and the wire diameter were concluded as compensation for the Nagaoka formula. Compared to conventional calculation formulas, the accuracy of the inductance calculation was improved by taking into account the structural characteristics of microsolenoids, including greater ratios of wire diameter and helix pitch to overall dimension. The derived formula was validated by measuring the inductance value of microsolenoids fabricated with a femtosecond-laser-based microsolidifying method and compared with the reported microcoil. Reliability and accuracy of the derived formula was maintained by evaluating the coefficients of determination $R^2$ and residual mean square. In addition, independent simulation groups were conducted during the curve-fitting process, which verified the reasonability and validity of the shape factors $\delta(\frac{H}{D})$ and $\varepsilon(\frac{H}{D})$ to correct the Nagaoka formula.

The derived formula focused on static inductance calculation of 3D microsolenoids. However, the current flows towards the inside of the coil at high frequencies; so the effective radius of the area where the current flows becomes smaller[16]. It is occasionally suggested to use the internal radius of the coil instead of the wire mean radius in the calculations in order to compensate for this effect. For densely-wound thin-wire uniform straight solenoids, the difference between the low- and high-frequency inductance is usually not large. For the 3D microsolenoids, more research should be undertaken for dynamic inductance prediction.

## Acknowledgment

This work is supported by the National Science Foundation of China under the Grant No. 61176113 and 51335008, the Special-funded program on national key scientific instruments and equipment development of China under the Grant No. 2012YQ12004706, the Program for Changjiang Scholars and Innovative Research Team in University (IRT1033).

## References

[1] RONG R, CHOI J W, and AHN C H. An on-chip magnetic bead separator for biocell sorting [J]. Journal of Micromechanics and Microengineering, 2006, 16 (12): 2783-2790.

[2] BADILITA V, KRATT K, BAXAN N, et al. On-chip three dimensional microcoils for MRI at the microscale [J]. Lab on a Chip, 2010, 11(10): 1387-1390.

[3] BAXAN N, KAHLERT U, MACIACZYK J, et al. Microcoil-based MR phase imaging and manganese enhanced microscopy of glial tumor neurospheres with direct optical correlation [J]. Magnetic Resonance in Medicine, 68(1): 86-97.

[4] LONG J R, COPELAND M. A. The modeling, characterization, and design of monolithic inductors for silicon RF IC's [J]. IEEE Journal of Solid-State Circuits, 1997, 32: 357-369.

[5] BRANDON E J, WESSELING E E, CHANG V, et al. Printed microinductors on flexible substrates for power applications [J]. IEEE Transactions on Components and Packaging Technologies, 2003, 26(3): 517-523.

[6] PIETERS P, Beyne E. Spiral inductors integrated in MCM-D using the design space concept [C]. Proceedings of IEEE International Conference on Multichip Modules and High Density Packaging, Denver, 1998, Apr: 478-483.

[7] SANTRA A, CHAKRABORTY N, Ganguly R. Analytical evaluation of magnetic field by planar micro-electromagnet spirals for MEMS applications [J]. Journal of Micromechanics and Microengineering, 2009, 19: 085018(10pp).

[8] CONWAY J T. Noncoaxial inductance calculations without the vector potential for axisymmetric coils and planar coils [J]. IEEE Transactions on Magnetics, 2008, 44(4): 453-462.

[9] Burghartz J N, Edelstein D C, Soyuer M, et al. RF circuit design aspects of spiral inductors on silicon [J]. IEEE Journal of Solid-State Circuits, 1998, 33:2028-2034.

[10] LONG J R. Monolithic transformers for silicon RF IC design [J]. IEEE Journal of solid-state circuits, 2000, 35(9): 1368-1382.

[11] NAGAOKA H. The Inductance Coefficients of Solenoids [J].J. Coll. Sci., 1909, 27:18-33.

[12] WHEELER H A. Inductance Formulas for Circular and Square Coils [J]. Proc. IEEE, 1982, 70 (12): 1449-1450.

[13] SHOULAIE A M A. Calculation and Measurement of Coil Inductance Profile in Tubular Linear Reluctance Motor and its Validation by Three Dimensional FEM [J]. Journal of Electrical Engineering, 62 (4): 220-226.

[14] TOMINAKA T. Inductance calculation for helical conductors [J].Superconductor Science and Technology, 2005, 18 (3): 214-222.

[15] LUNDIN R. A handbook formula for the inductance of a single-layer circular coil [J]. Proceedings of the IEEE, 1985, 73 (9): 1428-1429.

[16] GROVER F W. Inductance calculations: working formulas and tables [M]. 2004, Courier Dover Publications.

[17] BALDAN C A, FREITAS R C, HOMRICH R P, et al. Single layer cylindrical and helicoidal coil with voids between successive turns electromagnetic field calculation to be used in superconductor current limiter simulator for design purpose [J]. IEEE Transactions on Applied Superconductivity, 2004, 14(2): 796-799.

[18] YU D, HAN K. Self-inductance of air-core circular coils with rectangular cross section [J]. IEEE Transactions on Magnetics, 1987, 23(6): 3916-3921.

[19] TURNER R. Minimum inductance coils [J]. Journal of Physics E: Scientific Instruments, 1988, 21(10): 948-952.

[20] LU B, YANG X. Effects of High Frequency on the Distributed Parameters of the Sparse-Wound Solenoid Coils [J]. IEEE transactions on plasma science, 2014, 42(1): 154-161.

[21] PAHLAVANI M R A, SHOULAIE A A novel approach for calculations of helical toroidal coil inductance usable in reactor plasmas [J]. IEEE Transactions on Plasma Science, 2009, 37(8): 1593-1603.

[22] GYIMESI I, OSTERGAARD D. Inductance computation by incremental finite element analysis [J]. IEEE Transactions on Magnetics, 1999, 35(3): 1119-1122.

[23] LIU K, YANG Q, ZHAO Y, et al. Three-dimensional metallic microcomponents achieved in fused silica by a femtosecond-laser-based microsolidifying process [J]. Microelectronic Engineering, 2014, 113(1): 93-97.

[24] HE S, CHEN F, YANG Q, et al. Facile fabrication of true three-dimensional microcoils inside fused silica by a femtosecond laser [J]. Journal of Micromechanics and Microengineering, 1050. DOI: 10. 1088/0960 - 1317/22/10/105017.

## Authors' Biographies

**LIU Keyin**, born in 1987, is currently a doctor in the School of Mechanical Engineering, Xi´an Jiaotong University, China. He obtained his Bachelor of engineering degree from Xi´an Jiaotong University in 2010. His research direction is the femtosecond laser micromachining technology and microfluidic system.

E-mail: liukeyin@stu.xjtu.edu.cn

**YANG Qing**, is currently an associate professor in the State Key Laboratory for Manufacturing System Engineering, Xi'an Jiaotong University. She received her BS degree from Sichuan University in 1992, and PhD degree from Xi´an Institute of Optics and Precision Mechanics in 2009. Her research is focused on the femtosecond laser micromachining, microfluidic biochip and micro optics.

E-mail: yangqing@mail.xjtu.edu.cn

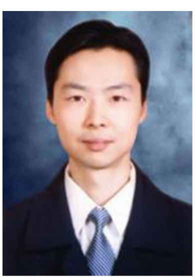

**CHEN Feng**, is currently a professor of Electronic Engineering at Xi´an Jiaotong University. Chen received the B. S. degree in physics from Sichuan University, China in 1991 and then began to work for Chinese Academy of Science (1991 to 2002). Chen received the Ph. D. in Optics from Chinese Academy of Science in 1997. He had been a Professor of Electronics Engineering at Xian Jiaotong University since 2002. His current research interests are femtosecond laser microfabrication and Bionic Microfabrication.

E-mail: chenfeng@mail.xjtu.edu.cn

**ZHAO Yulong**, received his B.S., M.S. and Ph. D. degrees in 1991, 1999 and 2003, respectively. Dr. Zhao is currently a professor of Xi'an Jiaotong University, China. His main research fields include MEMS sensors, biosensors, precise instrument and micro/nano manufacturing technology.

E-mail: zhaoyulong@mail.xjtu.edu.cn

**MENG Xiangwei**, received his BS in the Department of Electronic Science and Technology (2008) from Xi'an Jiaotong University. His research is focused on the fabrication of femtosecond laser wet etch and their applications in microfabrication, such as microcoils in lab-on-a-chip systems and micro-optical elements

E-mail: mxwgy@stu.xjtu.edu.cn

**SHAN Chao**, born in 1988, is currently a doctor in the School of Electronic and Information Engineering, Xi´an Jiaotong University, China. He obtained his Master degree from Xi´an Jiaotong University in 2014. His research direction is the femtosecond laser micromachining and a metal microsolidifying process to fabricate on-chip complex 3D microcoils.

E-mail: shanchaobest@sina.com

**LI Yanyang**, born in 1991, is currently a graduate student in the School of Mechanical Engineering, Xi'an Jiaotong University, China. His reaserch interests include Femtosecond laser hyperfine processing and Microfluidic chip, etc.

E-mail: liyanyang@stu.xjtu.edu.cn